Nanoparticle Hybrids

DOI: 10.1002/anie.201102911

Programming the Cellular Uptake of Physiologically Stable Peptide–Gold Nanoparticle Hybrids with Single Amino Acids**

*Hong Yang, Shan-Yu Fung, and Mingyao Liu**

The fast-developing field of nanotechnology has produced an enormous variety of nanoparticles (for example quantum dots, and metallic, magnetic, and polymeric nanoparticles) with different sizes and shapes for diverse biomedical applications in drug delivery, disease diagnostics, and medical imaging.[1] These nanoparticles often require surface modification to ensure their biocompatibility and/or enhance the bioavailability. In many cases, functional biomolecules, such as antibodies, peptides, and nucleic acid ligands, have been extensively introduced onto nanoparticles to enable cell-specific recognition, assist cellular uptake, and alter intracellular localization.[2] Thus, there is a tremendous need to fundamentally understand the interactions between these functionalized nanoparticles and biological systems, and how the nanoparticle surface chemistry affects the biological responses.

As part of this large scope, we developed a novel peptide–gold nanoparticle hybrid system to investigate the surface chemistry of the nanoparticles in determining their cellular responses. We selected the gold nanoparticle (GNP) as the core of the system for 1) its ease of surface modification by gold–thiol or gold–amine linkages; 2) the intrinsic fluorescence of GNP aggregates/clusters on surfaces for the direct observation of their cellular uptake by confocal or fluorescence microscopy;[3] and 3) clinical trials of GNPs in cancer therapy,[4] thus enabling our future development of the hybrid system for potential clinical uses.

The critical part of the hybrid system is the modulation of GNP surface properties by rationally designed peptide ligands (Supporting Information, Table S1). These peptide ligands contain three functional regions (Figure 1 a): the gold binding motif at the N terminus, the hydrophobic spacing region in the middle, and the functional end group at the C terminus. The gold binding motif consists of a cysteine (C) residue bearing a thiol group, together with the N-terminal amine group to form covalent linkages between the peptides and GNPs.[5] The middle region has four alanine residues (AAAA) to promote peptide assembly into a densely packed monolayer on the gold surface. The functional end group is a single amino acid, which can be positively charged arginine (P1) or lysine (P5), negatively charged glutamic acid (P2), neutral hydrophilic serine (P3), or hydrophobic tryptophan (P4). These end amino acids with different charge status, chemical structure, and hydrophobicity are expected to impart the GNP surface with corresponding properties.

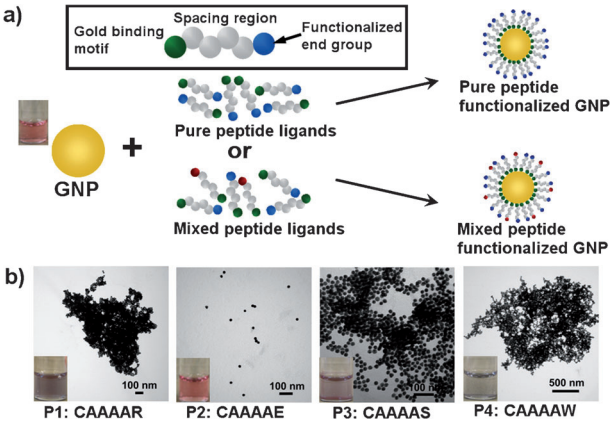

Figure 1. Preparation and characterization of peptide–GNP hybrids with different surface chemical properties. a) Peptide ligand design and peptide–GNP hybrid formulation strategies. b) TEM images of GNPs modified with various single peptide ligands (100 μM) in aqueous solution. Scale bars: 100 nm (P4: 500 nm).

The hybrid nanoparticles were constructed by modifying the gold surface with single peptide ligands or their binary mixtures. These hybrids were then assessed for their stability in aqueous solution, at the physiological ionic condition (150 mM NaCl) and with bovine serum albumin (BSA), the most abundant protein in serum. Only when peptide–GNP hybrids pass all the stability tests will they be further studied on the cellular responses.

Upon modifying the GNPs with single peptide ligands, we found that only P2 (with the negatively charged end glutamic acid) could stabilize GNPs in aqueous solution (Figure 1 b). The arginine-, serine-, and tryptophan-ended peptides (P1, P3, and P4) caused GNP aggregation (Figure 1 b), as did

[*] Dr. H. Yang, Dr. S. Y. Fung, Prof. M. Liu
Latner Thoracic Surgery Research Laboratories
University Health Network, Toronto General Research Institute
Toronto, Ontario, M5G 1L7 (Canada)
E-mail: mingyao.liu@utoronto.ca
Prof. M. Liu
Department of Surgery, Faculty of Medicine, University of Toronto
Toronto, Ontario, M5G 2C4 (Canada)

[**] We thank Steven Doyle, Battista Calvieri, and Yan Chen at the TEM facility center for technical assistance in cell embedding and TEM imaging. We acknowledge Prof. Gang Zheng for allowing the use of the instrument to conduct UV/Vis, DLS, and zeta potential experiments. We also thank Prof. Vladimir Baranov and Leslie Fung for help with ICP-MS measurements. We thank Feng Xu for help with confocal microscopy. S.Y.F. would like to acknowledge the Ontario Ministry of Research and Innovation and Michael V. Plachta and Wanda Plachta for providing a fellowship. The financial support of this project was from the Canadian Institutes of Health Research (MOP-13270 and MOP-42546).

Supporting information for this article is available on the WWW under http://dx.doi.org/10.1002/anie.201102911.

lysine-ended peptide (P5, data not shown). GNP aggregation can also be visualized by the change in solution color from red to purple or blue (Figure 1b, insets), owing to the change in surface plasma absorption.[5] This first screen narrowed our subsequent studies focusing on the negatively charged peptide–GNP hybrids.

To further change the surface chemistry of P2–GNPs, we formulated binary peptide mixtures by mixing P2 with other peptide ligands at certain molar ratios to modify GNPs. One formulation was the P2–P3 mixture to reduce the negative charges while maintaining the hydrophilicity; the other was the P2–P4 mixture to increase the hydrophobicity and introduce different chemical structures. By studying the stability (that is, aggregation) of various P2–P3 and P2–P4 mixtures at the physiological ionic condition (150 mM NaCl), we obtained four stable peptide–GNP hybrids: 100P2–GNP, 95P2P3–GNP, 90P2P3–GNP, and 95P2P4–GNP (Supporting Information, Figure S1a,b) (the number at the beginning of the names indicates the molar percentage of P2 in the mixtures). These stable hybrids were further challenged with high concentrations of NaCl to examine their differences. We found that their responses (stability: 100P2 ≈ 95P2P3 > 90P2P3 > 95P2P4 > GNP only) to the increasing salt concentration indeed reflected the differences in their surface ligand components (Supporting Information, Figure S1c). We then tested the interactions of the four stable peptide–GNP hybrids with BSA (10 μM in PBS) (Supporting Information, Figure S1d); they all showed good stability (less interaction) with BSA compared to the bare GNPs.

By changing only less than 10% peptide ligands (during modification), four peptide–GNP hybrids with different surface chemistry were generated. The question arises as to whether such a small difference would affect their cellular uptake, even though they all had similar stability, sizes, and surface charges (Supporting Information, Figure S1–S3). Human lung cancer A549 cells were used to address this question. We incubated the hybrids with A549 cells without serum for 3 h to study their cellular uptake. Interestingly, the uptake of these hybrids strongly depended on their surface chemistry by TEM imaging (Figure 2a–c), from a dramatically high uptake of 95P2P4–GNP to moderate (100P2–GNP) and minimal (95P2P3–GNP and 90P2P3–GNP) uptake; 90P2P3–GNP in particular almost had no uptake (data not shown). This uptake trend was also confirmed by confocal imaging (Supporting Information, Figure S4). To validate the results from these two imaging-based methods, we further quantified the number of peptide–GNPs internalized using inductively coupled plasma mass spectroscopy (ICP-MS; Figure 2d). With the treatment of 1 nM hybrids, we found that the uptake of 95P2P4–GNP, 100P2–GNP, and 95P2P3–GNP was 5×10^5/cell, 4×10^4/cell, and 6×10^3/cell, respectively. This trend was consistent with the TEM and confocal imaging results. Interestingly, the uptake of 95P2P4–GNP was found to be comparable with that of antisense oligonucleotide-modified GNP (ASNP, ca. 2.5×10^5/cell) in A549 cells,[6] although the experimental conditions in these two studies were different (13 nm GNP, 48 h with serum in Ref. [6] versus 20 nm GNP, 3 h without serum herein). In terms of their cellular localization, semiquantitative analysis (Figure 2b,c)

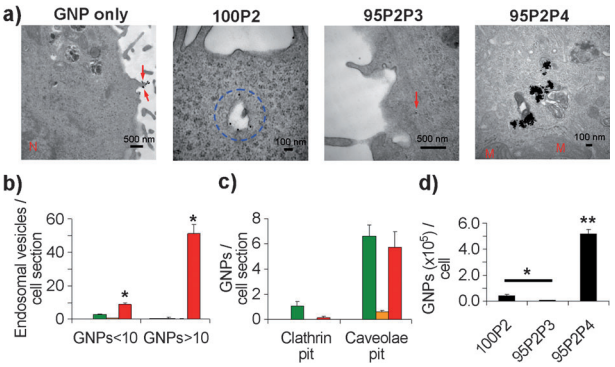

Figure 2. Uptake of the peptide–GNP hybrids into the human lung carcinoma A549 cells (in the absence of serum). a) Representative TEM images; red arrows indicate GNPs (black dots) in the cytoplasm or outside the cells; N nucleus; M mitochondria. Scale bars: 500 nm (GNP, 95P2P3), 100 nm (100P2, 95P2P4). b,c) Semiquantitative analysis of GNPs in different vesicles in the cells from TEM images (black: GNP only, green: 100P2–GNP, yellow: 95P2P3–GNP, red: 95P2P4–GNP). The analysis was performed over 30 cell sections for each group. ($\star$ $p < 0.05$, 95P2P4–GNP vs. all other groups). d) The number of internalized GNPs per cell analyzed by ICP-MS. ($\star$ $p < 0.05$ between 100P2 and 95P2P3; $\star\star$ $p < 0.05$ 95P2P4–GNP vs. all other groups). The error bar represents the SE.

showed that 100P2–GNPs were mainly in caveolae pits, whereas the majority of 95P2P4–GNPs were in endosomal/lysosomal vesicles (some in caveolae pits). In the presence of serum, bare GNPs showed the highest uptake, which is most likely due to the large adsorption of serum protein on the surface of GNPs. Nevertheless, the uptake of 95P2P4–GNPs remained the highest among the four hybrids (Supporting Information, Figure S5). This exciting discovery clearly demonstrated that small differences in ligands changed the surface chemistry of GNPs with tremendous impact on their cellular uptake.

Our next question was why the small difference in the modifying ligands (5% P4) dramatically enhances the hybrid uptake. We investigated three hypotheses: 1) The hydrophobic interaction between the end tryptophan of P4 and the cell membrane assists the internalization of the hybrids ("hydrophobicity hypothesis"); 2) the end aromatic structure plays an important role in regulating nanoparticle cellular uptake ("aromatic structure hypothesis"); and 3) the high uptake is specifically mediated by the tryptophan motif owing to its cell membrane anchoring and permeable capabilities ("tryptophan hypothesis").[7] To evaluate the first hypothesis, we point-mutated tryptophan of P4 to non-aromatic leucine (P6), isoleucine (P9), or valine (P10; Figure 3a). We found that such a mutation did not enhance the hybrid uptake as 95P2P4-GNP, but rather had similar uptake as 100P2–GNP (Figure 2 and Figure 3), indicating the hydrophobicity of the end amino acid was not critical to this event. We further substituted tryptophan to tyrosine (P7) and phenylalanine (P8) to test the "aromatic structure hypothesis" (Figure 3a). Interestingly, both substitutions enhanced the cellular uptake of GNPs by much more than that of 100P2–GNP (Figure 2 and Figure 3). However, their uptake was significantly lower than 95P2P4–GNP. These findings were confirmed by con-

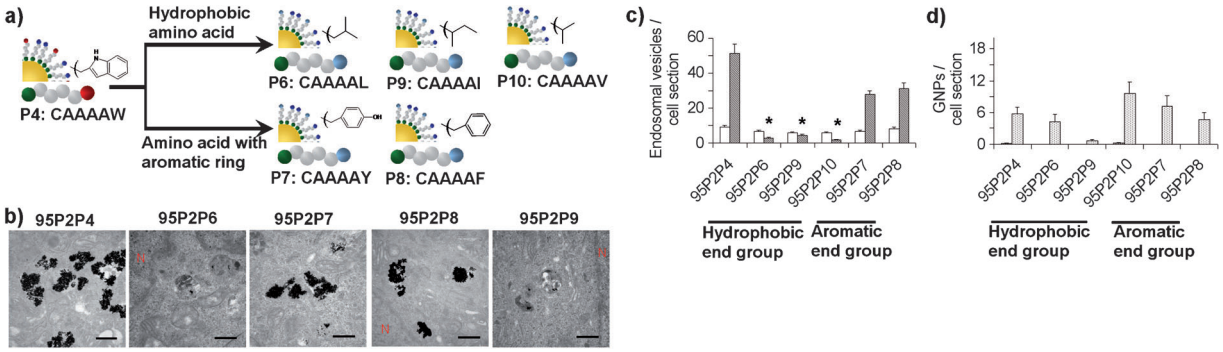

Figure 3. Enhanced cellular uptake of 95P2P4–GNP is mainly mediated by the end aromatic structure of tryptophan W on P4. a) Point mutation of tryptophan (P4) to hydrophobic amino acids leucine (P6), isoleucine (P9), and valine (P10) or aromatic amino acids tyrosine (P7) and phenylalanine (P8). b) Representative TEM images of selected groups. The scale bar represents 500 nm. The TEM images were further semi-quantitatively analyzed to determine c) the number of endosomal/lysosomal vesicles containing <10 GNPs (white bars) or >10 GNPs (shaded), and d) the number of GNPs in clathrin (hashed bars) or caveolae pits (dotted) per each cell section. The analysis was performed over 30 cell sections for each group. The error bar represents the SE ($\star\ p<0.05$, compared with 95P2P4–GNP group).

focal imaging (Supporting Information, Figure S6). The results suggested that the aromatic structures were essential to the enhanced uptake of the hybrids. One possible explanation was that upon interacting with cell membranes, these aromatic amino acids may induce membrane curvature and fusion with the lipid bilayer.[8] Among the three aromatic amino acids, tryptophan seems to be the most potent amino acid to enhance the cellular uptake of GNPs, which is possibly due to its high propensity for bilayer interaction.[9] Thus, we could not exclude the third hypothesis from our results.

In attempt to elucidate the mechanism of 95P2P4-GNP entry into A549 cells, we conducted uptake experiments at 4 °C and 37 °C and with different endocytosis inhibitors. First, we found that the uptake of 95P2P4–GNP at 4 °C was strongly

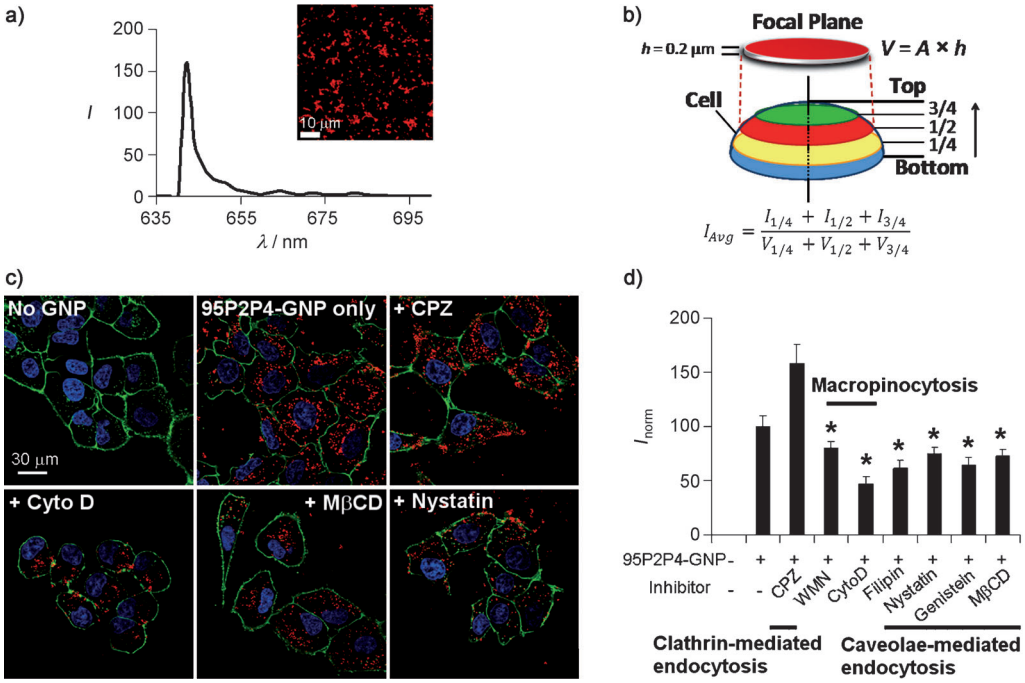

Figure 4. The endocytotic pathways of the 95P2P4–GNP uptake into A549 cells. a) Intrinsic fluorescence signals of 95P2P4–GNP aggregates formed at pH 4 with excitation at 633 nm; inset shows the confocal laser scanning microscope image of the aggregates emitting fluorescence at 645-655 nm. b) A cartoon showing the image analysis method to obtain average fluorescence signals (per volume) inside the cells; for each cell, three sections were selected at $z=1/4$, 1/2, and 3/4 of the cell thickness from the bottom; the volume of each section equals to the focal depth (setting at 0.2 μm) times the section area. c) Confocal fluorescence images of 95P2P4–GNPs in A549 cells pretreated with various endocytotic pathway inhibitors (CPZ, Cyto D, MβCD, and nystatin) in comparison with no inhibitor control and no GNP control; the cell membrane was stained with WGA-Alex Fluor 488, shown in green, and the GNP aggregates are shown in red; all images were captured at the same magnification. d) Quantitative analysis of the confocal images to show the inhibitory effect on the 95P2P4-GNP uptake. The error bar represents the SE ($\star\ p<0.05$, compared with no inhibitor group).

reduced compared to 37 °C, indicating that the entry of 95P2P4–GNP was mainly by energy-dependent processes (Supporting Information, Figure S7). We then performed inhibitory experiments using confocal imaging to monitor the intrinsic fluorescence (645–655 nm) of the GNP aggregates (Figure 4a) in the cells.[3] The cell membrane was stained with WGA–Alex Fluor 488 to quantify the GNP fluorescence signals inside the cell. The average uptake signals were determined using the method shown in Figure 4b. From the images and quantitative analysis (Figure 4c and d), we found that the macropinocytosis inhibitors WMN and CytoD, and the caveolae/lipid raft-mediated endocytosis inhibitors filipin, nystatin, genistein, and MβCD were able to significantly reduce the 95P2P4–GNP uptake, but not the clathrin-mediated endocytosis inhibitor CPZ.

These results not only demonstrate the possible endocytotic pathways of 95P2P4-GNP uptake, but also provide evidence supporting the speculations of membrane anchoring and curvature formation in relation to the P4-enhanced cellular uptake of 95P2P4–GNPs. CytoD can disrupt F-actin filaments by actin depolymerization; genistein (a tyrosine kinase inhibitor) can inhibit actin recruitment in caveolae. Therefore, these two inhibitors could disturb the membrane curvature formation and fusion by which the end tryptophan of P4 is utilized to enhance 95P2P4–GNP internalization. The depletion of cholesterol in the cell membrane by filipin and MβCD, and the disruption of lipid rafts by nystatin (cholesterol binding), could also prevent the interaction of 95P2P4–GNP with membrane lipids. This is most likely the reason we observed an inhibitory effect from all of the studied inhibitors except CPZ. These observations also imply that the site of action for 95P2P4-GNP internalization is at the cholesterol-rich regions, where the affinity of the aromatic ring structure of tryptophan on GNPs with the ring-like structure of cholesterol could cause membrane curvature and fusion, leading to dramatically enhanced cellular uptake of nanoparticles.

In conclusion, we successfully constructed novel, physiologically stable peptide–GNP hybrids with different surface chemical properties. Furthermore, we showed that the chemical and structural properties of the hybrid surface are critical for regulating their cellular uptake. By altering only 5–10% of the end amino acids of the peptide ligands from glutamic acid to tryptophan or serine, the uptake of GNPs can be dramatically increased or suppressed to minimum, respectively. The enhanced uptake of 95P2P4–GNPs was related to the aromatic structure of the end tryptophan of P4 involved in membrane anchoring and permeation. This work provides insights into the role of nanoparticle surface chemistry in determining the cellular uptake event, which will further aid to the development of peptide–GNP hybrids as efficient diagnostic tools and effective therapeutics in future medicine.

Received: April 27, 2011

Keywords: amino acid mutation · cellular uptake · nanoparticles · peptides · surface structure

[1] a) A. Verma, F. Stellacci, *Small* **2010**, *6*, 12–21; b) C. C. You, O. R. Miranda, B. Gider, P. S. Ghosh, I. B. Kim, B. Erdogan, S. A. Krovi, U. H. F. Bunz, V. M. Rotello, *Nat. Nanotechnol.* **2007**, *2*, 318–323; c) J. H. Park, L. Gu, G. von Maltzahn, E. Ruoslahti, S. N. Bhatia, M. J. Sailor, *Nat. Mater.* **2009**, *8*, 331–336; d) Y. Wang, S. Gao, W. H. Ye, H. S. Yoon, Y. Y. Yang, *Nat. Mater.* **2006**, *5*, 791–796; e) E. Tasciotti, X. Liu, R. Bhavane, K. Plant, A. D. Leonard, B. K. Price, M. M. Cheng, P. Decuzzi, J. M. Tour, F. Robertson, M. Ferrari, *Nat. Nanotechnol.* **2008**, *3*, 151–157; f) J. Dobson, *Nat. Nanotechnol.* **2008**, *3*, 139–143.

[2] a) N. L. Rosi, D. A. Giljohann, C. S. Thaxton, A. K. R. Lytton-Jean, M. S. Han, C. A. Mirkin, *Science* **2006**, *312*, 1027–1030; b) B. Kim, G. Han, B. J. Toley, C. Kim, V. M. Rotello, N. S. Forbes, *Nat. Nanotechnol.* **2010**, *5*, 465–472; c) W. Jiang, B. Y. Kim, J. T. Rutka, W. C. Chan, *Nat. Nanotechnol.* **2008**, *3*, 145–150.

[3] C. D. Geddes, A. Parfenov, I. Gryczynski, J. R. Lakowicz, *Chem. Phys. Lett.* **2003**, *380*, 269–272.

[4] a) G. F. Paciotti, L. Myer, D. Weinreich, D. Goia, N. Pavel, R. E. McLaughlin, L. Tamarkin, *Drug Delivery* **2004**, *11*, 169–183; b) G. Paciotti, D. G. I. Kingston, L. Tamarkin, *Drug Dev. Res.* **2006**, *67*, 47–54.

[5] R. Levy, N. T. Thanh, R. C. Doty, I. Hussain, R. J. Nichols, D. J. Schiffrin, M. Brust, D. G. Fernig, *J. Am. Chem. Soc.* **2004**, *126*, 10076–10084.

[6] D. A. Giljohann, D. S. Seferos, P. C. Patel, J. E. Millstone, N. L. Rosi, C. A. Mirkin, *Nano. Lett.* **2007**, *7*, 3818–3821.

[7] a) D. Derossi, A. H. Joliot, G. Chassaing, A. Prochiantz, *J. Biol. Chem.* **1994**, *269*, 10444–10450; b) M. Magzoub, L. E. Eriksson, A. Graslund, *Biophys. Chem.* **2003**, *103*, 271–288.

[8] a) S. Martens, H. T. McMahon, *Nat. Rev. Mol. Cell Biol.* **2008**, *9*, 543–556; b) C. A. Helm, J. N. Israelachvili, P. M. McGuiggan, *Science* **1989**, *246*, 919–922; c) C. A. Helm, J. N. Israelachvili, P. M. McGuiggan, *Biochemistry* **1992**, *31*, 1794–1805; d) A. Walrant, I. Correia, C. Jiao, O. Lequin, E. H. Bent, N. Goasdoue, C. Lacombe, G. Chassaing, S. Sagan, I. D. Alves, *Biochim. Biophys. Acta Biomembr.* **2011**, *1808*, 382–393.

[9] F. Seiler, J. Malsam, J. M. Krause, T. H. Sollner, *FEBS Lett.* **2009**, *583*, 2343–2348.

